



Open Archive TOULOUSE Archive Ouverte (OATAO)

OATAO is an open access repository that collects the work of Toulouse researchers and makes it freely available over the web where possible.

This is an author-deposited version published in : <http://oatao.univ-toulouse.fr/>
Eprints ID : 16020

To link to this article : DOI:10.2514/6.2016-4612
URL : <http://dx.doi.org/10.2514/6.2016-4612>

To cite this version : Thauvin, Jérôme and Barraud, Guillaume and Budinger, Marc and Leray, Dimitri and Roboam, Xavier and Sareni, Bruno *Hybrid Regional Aircraft: A Comparative Review of New Potentials Enabled by Electric Power*. (2016) In: 52nd AIAA/SAE/ASEE Joint Propulsion Conference, 25 July 2016 - 27 July 2016 (Salt Lake City, United States).

Any correspondence concerning this service should be sent to the repository administrator: staff-oatao@listes-diff.inp-toulouse.fr

Hybrid Regional Aircraft: A Comparative Review of New Potentials Enabled by Electric Power

Jérôme Thauvin¹ and Guillaume Barraud²
Airbus Operations SAS, Toulouse, 31060, France

Marc Budinger³ and Dimitri Leray⁴
Institut Clément Ader (ICA, UMR CNRS 5312), Université de Toulouse, 31400, Toulouse, France

and

Xavier Roboam⁵ and Bruno Sareni⁶
LAPLACE(CNRS/INPT/UPS), Université de Toulouse, 31071, Toulouse, France

This article assesses the benefits of hybridization within the regional aircraft scale using a conventional twin-turbo propeller aircraft as reference. For a fair comparison, this reference aircraft was designed assuming a 2035 technology level. The propulsion system of the reference aircraft is analyzed along the mission and the phases of flight with low efficiencies are highlighted. Then the potential benefits of new power management through the use of secondary power generation systems but also through the variation of the size of prime movers are presented and discussed. In particular, the effect of the gas turbine size on its efficiency is studied. Finally, the article focuses on aerodynamic improvements enabled by new propeller or fan integrations and the associated concepts such as differential thrust, blown wing and boundary layer ingestion. For each topic, simplified analyses provide estimated potential of energy saving. These results can be used as indicators for selecting the most promising hybrid architecture concepts for a regional aircraft.

Nomenclature

BE	=	Block Energy
BF	=	Block Fuel
BLI	=	Boundary Layer Ingestion
C_P	=	propeller power coefficient
C_T	=	propeller thrust coefficient
D	=	propeller diameter
D_F	=	fuselage drag
FL	=	Flight Level
ISA	=	International Standard Atmosphere
J	=	propeller advance ratio
MLW	=	Maximum Landing Weight
MTOW	=	Maximum Take-Off Weight
MZFW	=	Maximum Zero Fuel Weight
\dot{m}_{BL}	=	mass flow rate in the fuselage wake
\dot{m}_p	=	mass flow rate through propeller disk

¹ Ph.D. Student, Future Projects Office, 316 route de Bayonne, Cedex 9, AIAA Member.

² Aerospace Engineer, Future Projects Office, 316 route de Bayonne, Cedex 9.

³ Associate Professor, 135 avenue de Rangueil, Cedex 4, AIAA Member.

⁴ Associate Professor, 135 avenue de Rangueil, Cedex 4.

⁵ Senior Researcher, 2 Rue Camichel.

⁶ Professor, 2 Rue Camichel.

n	=	propeller rotation per second
N_p	=	maximum propeller speed
OEW	=	Operating Empty Weight
P	=	propeller shaft power
P_k	=	kinetic power imparted to flow
p_∞	=	freestream static pressure
PSFC	=	Power Specific Fuel Consumption
R_{CC}	=	fuselage radius at section CC
SL	=	Sea Level
S_p	=	propulsor disk area
T	=	propeller thrust
T_p	=	propulsor thrust
T_4	=	gas turbine design temperature (high pressure turbine inlet temperature)
V	=	aircraft speed
v_{BL}	=	equivalent uniform velocity in the fuselage wake
v_e	=	axial velocity in propeller slipstream
v_∞	=	freestream velocity
v_m	=	fluid velocity after iso-momentum mixing
δ	=	boundary layer thickness
η	=	propeller efficiency
ρ	=	air density

I. Introduction

PROPULSION system innovations have been a key driver of aeronautic evolution. The increase of propulsion performance and efficiency has enabled aircraft to travel at higher speeds over longer ranges while carrying larger payloads. Today the improvement of conventional engine technologies is reaching an asymptote, while future demands on the air transport systems still dictate that aircraft should be less polluting, less noisy and more fuel efficient. In this context, hybrid architectures offer the opportunity to transform in the long term the landscape of aircraft propulsion and furthermore enable new aircraft configurations.

In this article the term hybrid aircraft is used to define an aircraft that operates more than one type of energy source and/or power flow for propulsion means. Aircraft propulsion is indeed currently limited to kerosene and mechanical transmissions. Hybrid electric propulsion provides the opportunity to combine different energy sources or power flows by integrating new technology bricks. Those give additional degrees of freedom to improve overall aircraft performance, limit the use of non-renewable fossil resources and reduce the aircraft environmental footprint.

Today, hybrid technology has mainly been applied to ground-based transports, cars, buses and trains but also ships. However, the feasibility of hybrid architectures in the air industry has to be established and the improvement in aircraft performance has still to be demonstrated.

This paper aims to review the new energy saving opportunities enabled by electric power in the case of a regional aircraft. These opportunities are evaluated with respect to a reference conventional aircraft that was designed for the purpose of this study.

II. Reference Aircraft and Reference Engine

The reference aircraft is a conventional twin-turbo propeller, designed under the requirements listed in Table 1. Also, for a fair comparison, this reference aircraft was designed assuming a 2035 technology level. The engine size and the reference area are constrained by the time to climb and the approach speed. Specifications of the reference aircraft are shown in Table 2 and the aircraft is illustrated in Fig. 1.

Table 1. Aircraft design requirements.

Number of passengers	70 pax
Range capability	400 nm
Cruise altitude	20,000 ft
Cruise Mach number	0.45
Time to climb	17 min
Take-off field length (@MTOW, SL, ISA+15)	1400 m
Approach speed (@MLW, SL, ISA)	113 kt



Figure 1. Reference aircraft.

Table 2. Aircraft characteristics.

Wing Geometry	
Reference area	60.2 m ²
Aspect ratio	12
Design Weights	
MTOW	20,520 kg
MLW	21,113 kg
MZFW	19,517 kg
OWE	12,843 kg
Aerodynamic	
Max. lift-to-drag ratio	17.4
Propulsion	
Max. take-off power	2470 shp
Max. cruise power	2110 shp
Cruise PSFC (@19,900kg, ISA)	0.166 kg/h/shp
Off-takes	Mechanical
6-bladed propeller diameter	3.93 m

Despite the range capability of 400 nm, the aircraft performance is evaluated on a 200 nm mission (Table 3) as this aircraft is expected to operate most of its life on such range.

Table 3. Mission overview.

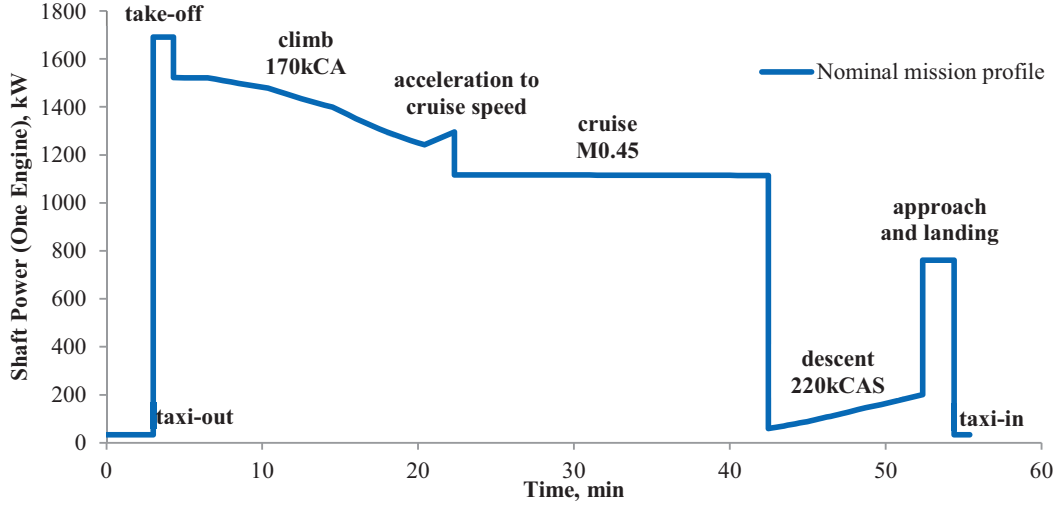
Phase	Time (min)	Distance (nm)	Fuel (kg)	% Block Fuel
Taxi out	3.0	0.0	9	2.0%
Take-off	1.3	0.0	21	4.8%
Climb	16.1	54.6	177	40.0%
Cruise	22.0	101.0	186	42.1%
Descent	9.9	44.4	32	7.2%
Approach and Landing	2.0	0.0	14	3.2%
Taxi in	1.0	0.0	3	0.7%
Total	55.3	200.0	442	100.0%

The reference aircraft is fitted with two turbopropeller engines of 3500 thermal horsepower each. A two spool architecture was selected as it provides a better combination of low complexity, light weight and low maintenance costs than a three-spool engine. The high-pressure spool comprises an axial compressor combined to a centrifugal compressor and a high pressure turbine driving the compressor stages. The combination of axial and centrifugal compressors offers a good compromise between high pressure ratio, high efficiency and limited length. A higher level of efficiency can theoretically be reached by a full axial compressor of same pressure ratio but the blade height of the last stages would be so small that flow turbulence imparted by required clearance between blade tips and casing would degrade its performance. The high-pressure spool also incorporates handling bleed valves that are used only in case of overload in particular during idle operations. The low pressure-shaft consists of a low pressure turbine driving the propeller gearbox. This engine features mechanical off-takes: the propeller gearbox drives an alternator and the accessory gearbox that is linked to the high-pressure shaft drives a starter generator.

From this architecture the possibilities in terms of number of stages for the turbines and compressor, shaft speeds, overall pressure ratio and core size are many and varied. The engine has been modeled and optimized under an in-house tool dedicated to engine preliminary design and based on published component maps. The main engine requirements at design point are described in Table 4. The resulting overall pressure ratio is 22 and the core size, defined as the air inlet flow corrected by the conditions at the outlet of the centrifugal high pressure compressor is 0.61 kg/s. Also, Fig. 2 provides the power profile of this reference engine along the 200 nm mission.

Table 4. Engine design requirements.

Shaft power	1770 shp
Design Altitude	20,000 ft
Temperature	ISA+10
Design Mach number	0.45
Power off-takes - propeller gearbox	80 shp
Power off-takes - accessory gearbox	15 shp

**Figure 2. Power profile of the reference aircraft.**

III. Power Management and Efficiency

Tackling the problem of low efficiency in certain phases of the mission should lead to immediate fuel savings. This section focuses on propeller and gas turbine efficiency. The propulsion system of the reference aircraft will be analyzed using the operating points indicated in Table 5.

Table 5. Total thrust for nominal mission.

Phase	Code	Altitude (ft)	Mach	Total thrust (N)
Taxi	TX	0	0.02	4021
Take-Off	TO	1500	0.18	46,000
Climb	CL	10,000	0.31	25,300
Cruise	CR	20,000	0.45	13,900
Descent	DSC	10,000	0.39	-300

A. Propeller Efficiency

On current turboprop aircraft, propellers are “constant-speed” propeller meaning that the propeller rpm is constant during each phase of flight. A hydraulic propeller pitch changing mechanism adjusts the blade pitch to keep the propeller rpm to the required value. The idle speed is generally never under 60% of the maximum propeller speed N_p due to the minimum frequency required by non-propulsive systems and other hydraulic power generation equipment connected to the gearbox. The propeller efficiency maps of the reference aircraft (Fig. 3) are derived from a typical efficiency map of Ref. 1 rescaled according to the number of blades. The performance parameters used in these maps are defined by:

$$\text{Advance Ratio:} \quad J = V/(nD) \quad (1)$$

$$\text{Power coefficient:} \quad C_p = P/(\rho n^3 D^5) \quad (2)$$

$$\text{Thrust coefficient:} \quad C_T = T/(\rho n^2 D^4) \quad (3)$$

$$\text{Propeller efficiency:} \quad \eta = J C_T / C_P \quad (4)$$

The red dots locate the propeller operating point in the conditions listed before (Table 5). To place them, an optimization was performed in order to maximize the propeller efficiency by varying the propeller speed between $60\% N_p$ and $100\% N_p$ and the blade pitch angle to reach the given propeller thrust. One can notice that the propeller efficiencies in climb and in cruise are very good while the efficiency in taxi is almost three times less. TX-2p refers to taxiing with two propellers while TX-1p refers to the single propeller taxi case. Performing the taxi using one propeller instead of two slightly increases the efficiency from 31% to 35%. The main advantage of single propeller taxi on current aircraft is mainly due to the poor efficiency of the gas turbine in idle and only incidentally to the increase of propeller efficiency as shown in the next section. For both taxi cases the propeller rpm was driven by the optimizer to the lower bound $60\% N_p$. Using hybrid-electric systems during taxi should enable to release this minimum speed constraint. A new set of calculations have been done for the taxi cases by removing the lower bound on propeller rpm. The new propeller efficiencies are located by the green dots in Fig. 3. Enabling the propeller to rotate slower than $60\% N_p$ increases the propeller efficiency by at least 7% for the single propeller taxi (41% efficiency). It is also noticeable that the propeller efficiency is now higher when the thrust for taxi is equally shared between the propellers as it reaches 52%.

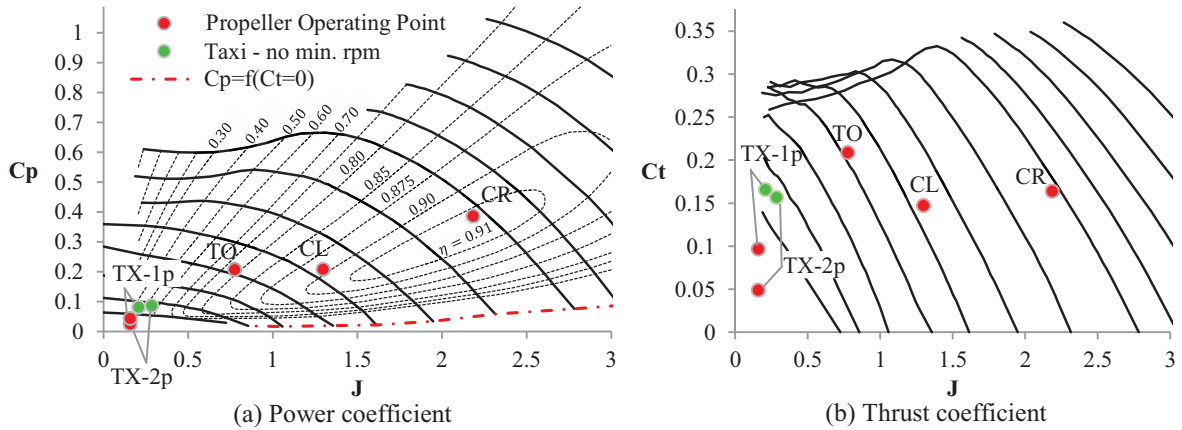


Figure 3. Propeller performance maps of the reference aircraft. Solid lines are constant blade pitch angle lines.

Table 6. Summary of “Low Propeller rpm in Taxi” analysis.

Benefits	<ul style="list-style-type: none"> ▪ Propeller efficiency increased by 49%.
Penalties	<ul style="list-style-type: none"> ▪ Non-propulsive systems (including hydraulic power generation) to be rethought. ▪ Possible weight penalties imparted by new components (electromechanical actuators, power electronics, etc...).

B. Engine Operating Point

The efficiency map of the reference engine under cruise conditions is shown in the torque-speed coordinate system in Fig. 4. It is obvious that the turboshaft provides its best specific fuel consumption when operating at its maximum output power capability, that is, at the design power. The operating area is limited on the high torque region by the maximum allowable temperature T_4 at the inlet of the high pressure turbine while the high speed region is bounded by mechanical strength (e.g. centrifugal constraints). In order to get the best efficiency of the gas turbine in cruise, the output speed must be kept constant and equal to the maximum allowable continuous speed whatever the output power: the constant speed propeller enables to do so. However, the gas turbine size can be driven by take-off or climb capability requirements, which is the case for the reference aircraft. The engine is therefore oversized for the reference cruise altitude leading to torque level in cruise less than the optimum efficiency level. This power gap is noticeable between the acceleration segment and the cruise of Fig. 2. Climbing to a higher

cruise altitude may slightly reduce this gap. An alternative would be to downsize the gas turbine and provide power boost to meet the limiting design requirements through an additional power generation system. Of course the effect of the additional weight of this secondary power generation is to be taken into account when evaluating overall cruise performance. Also, the effect of the gas turbine size on its efficiency is to be considered and will be addressed in part D.

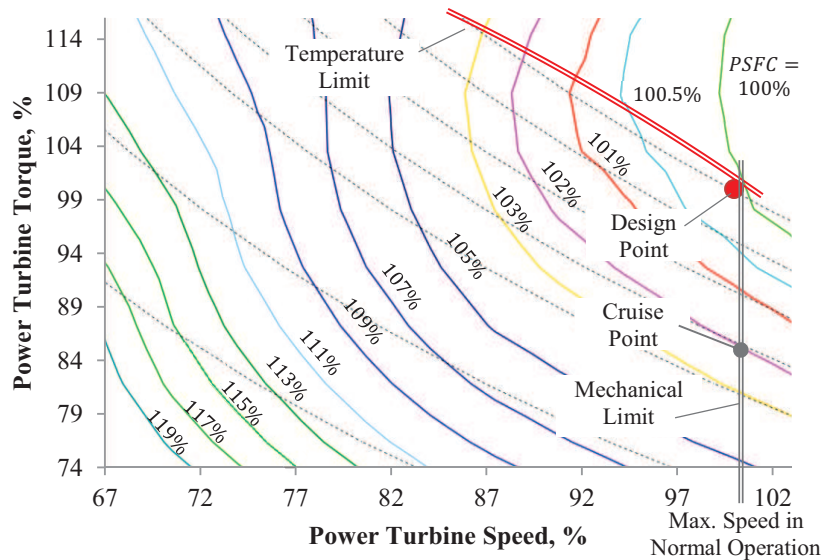


Figure 4. Gas turbine efficiency map in cruise (FL200, ISA, M0.45).
Dashed lines are constant output power lines.

If the gas turbine efficiency is good during high power demand phases, the picture changes when it comes to idle operations. Figure 5 shows the gas turbine efficiency map under typical taxi conditions. Contrary to the cruise case, the efficiency is roughly independent of the output speed for a given output power. For a 60% output speed, increasing the output torque from 8%—the power required for two propeller taxi—to 16%—the power required for single propeller taxi—reduces the specific fuel consumption by a factor of 1.8, which confirms that the single engine taxi is preferred to reduce fuel burn. Yet the gas turbine efficiency is still more than 5 times poorer than at the design point. In flight idle rating, the efficiency of the gas turbine is in the same order of magnitude as in taxi.

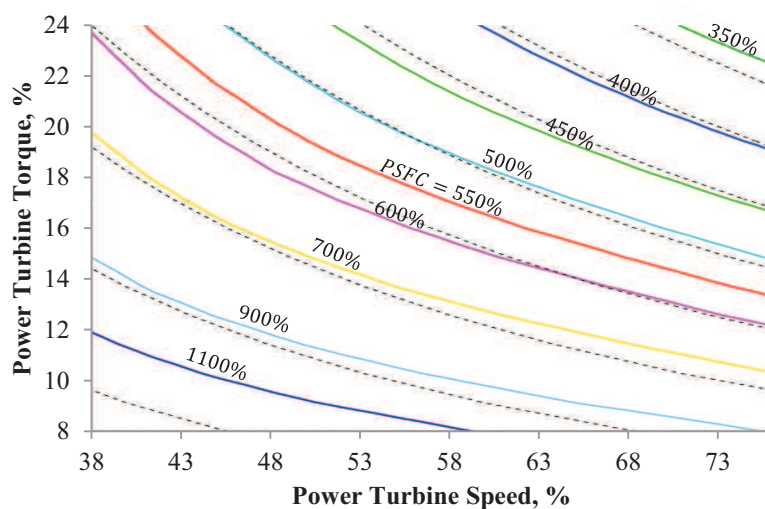


Figure 5. Gas turbine efficiency map in taxi (SL, ISA, M0.02).
Dashed lines are constant output power lines.

This leads us to consider two options to decrease the energy consumption in low efficiency phases of a gas turbine: modify the number of prime movers and/or add secondary energy sources.

C. Secondary Energy Source: Start and Stop

The start and stop function is now being used in most of hybrid vehicles. In particular, to allow the internal combustion engine to be switched off at a stop, the air conditioning system had to be redesigned and is now powered by batteries. Batteries are also used in some hybrid ship architecture. The additional battery power is then available for slow speed transits in harbour (diesel engine is then turned-off) or for peak power load smoothing. Assuming that this start and stop function can be mature and reliable enough, including rapid re-activation of the gas turbine², the descent could be flown with the gas turbines off as far as non-propulsive systems are provided by a secondary power generation system. In the same way, taxi phases could be performed on a full electric mode. Batteries or fuel cells³ are usual candidates as secondary power sources. Reference 4 shows a potential benefit of 60% on energy consumption for descent phase.

Table 7. Summary of “Secondary Energy Source for Start and Stop” analysis.

Benefits	<ul style="list-style-type: none"> ▪ Energy consumption in descent decreased by 60%. ▪ Energy consumption in taxi decreased by 90% (<i>assuming 90% efficiency of the electrical system vs. 10% of conventional gas turbine in ground idle</i>).
Penalties	<ul style="list-style-type: none"> ▪ Non-propulsive systems to be redesigned (Environmental Control System, Anti-icing, etc...). ▪ Additional weight of secondary energy source.

D. Number of Prime Movers and Size Effect

Some hybrid ship propulsion systems are characterized by their high number of diesel generators. The number of running generators depends on the required power, ensuring that diesel generators operate at an optimum efficiency throughout the cycle.

In order to assess the effect of the gas turbine size on its efficiency, two other turboshafts were designed with the use of the in-house engine preliminary design tool. Under the design conditions of Table 4, these turbines provide 1500 shp and 3540 shp output power, respectively. The same architecture as the reference engine (1770 shp) is considered for both turbines. For simplicity, design parameters such as tip-speeds, pressure ratio split between axial and centrifugal compressors and number of stages for the compressor and turbines were kept constant from the reference engine. However, design temperature T_4 was optimized. While the 1770 shp and 1500 shp engines have similar core sizes, the 3540 shp core size is increased by 80%. Specific fuel consumptions at design point for the three turbines are shown in Fig. 6.

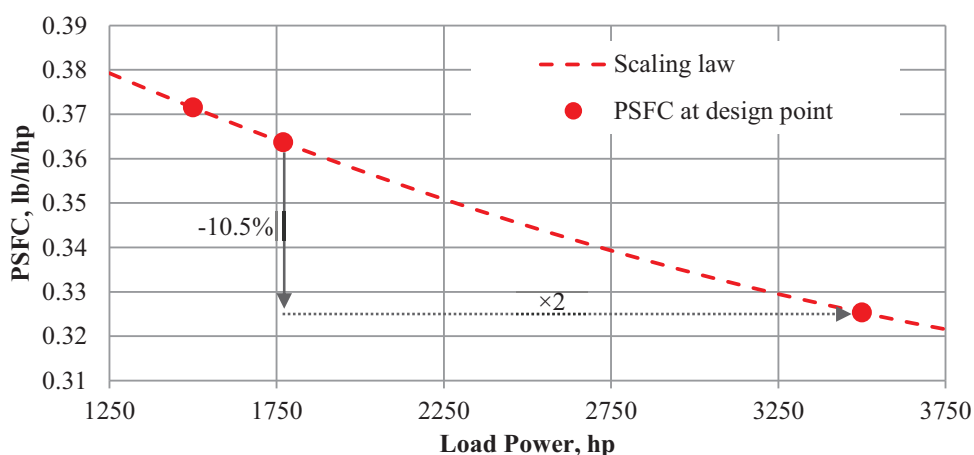


Figure 6. Size effect on gas turbine efficiency at design point (FL200, ISA+10, M0.45).

It is clear that the bigger the gas turbine, the more efficient. As an example, using one big 3540 shp gas turbine instead of two 1770 shp gas turbines enables to save 10.5% on the prime mover efficiency at design point. However, having a single turbine in nominal operation requires a back-up system sized to cope with the failure of this turbine

and capable of providing roughly half the nominal aircraft power to ensure same flight capabilities as the reference aircraft.

Table 8. Summary of “Single Engine Aircraft” analysis.

Benefits	▪ Prime mover efficiency increased by 10.5%.
Penalties	▪ Additional weight of back-up system.

The effect of gas turbine downsizing mentioned in part B can also be commented thanks to this study. As the reference engine is sized by the time-to-climb constraint, the cruise power is approximately 14% less than the design power at cruise level (Fig. 7).

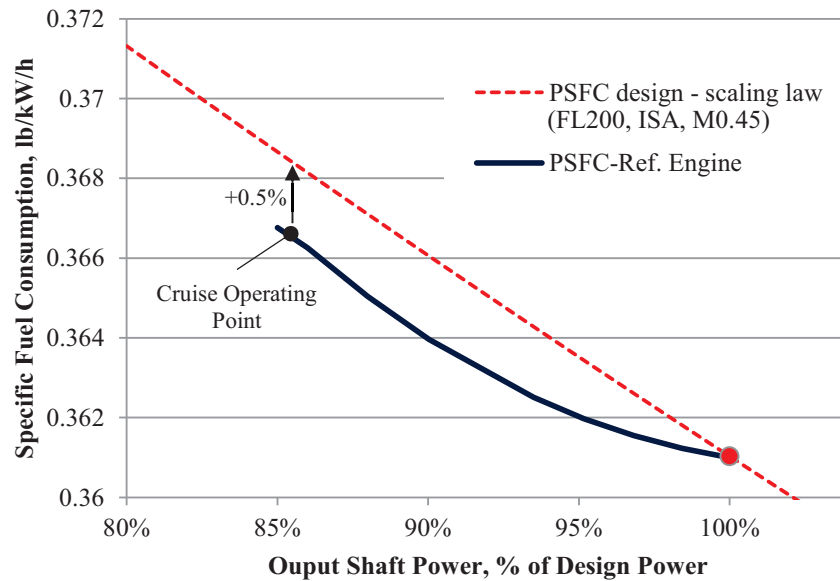


Figure 7. Cruise efficiency of reference engine and effect of engine downsizing.

If the engines are designed for the cruise power only, then we can reasonably assume that the secondary power generation system added to the aircraft will at least compensate the weight reduction due to the engine downsizing. Considering that the overall weight and other aerodynamic characteristics are unchanged in best case scenario, the required power for cruise is the same. Consequently the new engine design point can be placed along the red dashed line representing the scaling law discussed previously. This results in a 0.5% penalty on the specific fuel consumption that will be imparted to the block fuel.

At first sight, the interest of gas turbine downsizing is limited regarding the engine efficiency and the added weight of the secondary power generation system that will penalize even further the aircraft through the snow ball effects at aircraft level. However, these penalties are to be mitigated to some extent as engine integration is made easier and engine maintenance costs may be reduced.

Table 9. Summary of “Engine Downsizing” analysis.

Benefits	▪ Lower maintenance costs. ▪ Easier engine integration.
Penalties	▪ Prime mover efficiency reduced by 0.5%. ▪ Additional weight of secondary power generation system.

E. Energy Recovering

The opportunity of recovering energy in descent (using propeller in windmilling mode) and during landing (with braking systems) has been analyzed in Ref. 3 but has not proven to bring benefit on a hybrid aircraft. Propellers in windmilling mode create additional drag affecting the overall mission profile while the kinetic energy that could be recovered at landing is small compared to the overall energy consumption, not to mention the added system complexity as it should be able to withstand very high power flows during the landing phase.

Table 10. Summary of “Energy Recovering” analysis.

Benefits	<ul style="list-style-type: none"> ▪ Maximum recoverable kinetic energy at landing=0.19% BE.
Penalties	<ul style="list-style-type: none"> ▪ Increased Block Energy for energy recovering in descent. ▪ System complexity for kinetic energy recovering at landing. ▪ Additional weight of energy recovering systems.

IV. Aerodynamics

Driving wheels, propellers or fans electrically instead of mechanically provides great flexibility as far as locating is concerned. Electrical power is thus a key enabler for distributed propulsion. This part will analyse distributed electric propulsion solutions for the reference aircraft and discuss the improvements of aerodynamic efficiency related to: differential thrust, blown wing and boundary layer ingestion.

A. Differential Thrust

While the transient response of gas turbines is in the order of a few seconds, the use of hybrid propulsion system and electric motors to drive the propellers could enable to drastically decrease the thrust response time⁵. If the dynamic response is fast enough then helping the vertical tail plane of the aircraft to control the yaw moment with differential thrust appears possible.

The vertical tail plane of a conventional aircraft is sized to give yaw stability and controllability. The rudder must be able to counter the yaw moment generated by the asymmetric thrust in case of engine failure. The sizing conditions are generally at take-off, when the air speed is low and the remaining engines are at full power. Also, the vertical tail plane must be able to provide enough Dutch roll stability. This mode of oscillations is a complex coupling between Yaw and Roll motions. Finally, the aircraft should not be too stable: the rudder must provide crosswind capability in order to align the aircraft with the runway prior to landing in such conditions.

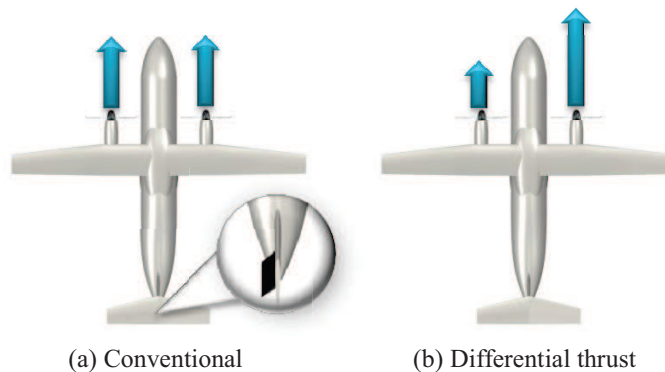


Figure 8. Illustration of yaw control.

Using differential thrust is thus an opportunity to shrink the vertical tail leading to a reduction of the aircraft friction drag. In order to assess the maximum aerodynamic benefit of this surface reduction, the vertical tail plane of the reference aircraft was totally removed and the drag polar updated accordingly. The performance of this aircraft was analyzed without accounting for any weight saving nor engine resizing versus the reference aircraft. The calculation shows around 6% reduction in fuel burn. If such aircraft would exist, the controllability and stability of the yaw moment would entirely rely on the propulsion system and its capability of providing a minimum amount of differential thrust in case of component failure. Even if the potential energy saving is attractive, the right balance between vertical tail plane shrinkage and amount of differential thrust used is to be studied further into details as a function of safety requirements.

Table 11. Summary of “Differential Thrust” analysis.

Benefits	<ul style="list-style-type: none"> ▪ -6% Block Energy (with fully removed fin).
Penalties	<ul style="list-style-type: none"> ▪ Reduced aircraft natural stability.

B. Blown Wing

The reference area of an aircraft is generally sized by low speed performance requirements such as take-off field length and approach speed and depends on the choice of high lift devices. In particular for the reference aircraft, the resulting reference area is not optimized for cruise performance: the lift coefficient in cruise is smaller than the lift coefficient of best lift-to-drag ratio. The cruise is therefore not flown at best aerodynamic efficiency. Turbofan aircraft can generally achieve their cruise at best lift-to-drag ratio by flying at higher altitudes. In the case of the reference aircraft, climbing to a much higher altitude has little sense as the range is small and bigger engines would be required. Therefore having a smaller wing in cruise would increase the aerodynamic efficiency of the reference aircraft. To do so, one can upgrade the high-lift systems by more complex devices. With the most complex unpowered high-lift devices, such as slats plus multiple slotted fowler flaps, the maximum lift coefficient reaches 3. But higher level of maximum lift capacity can be achieved with powered high-lift devices. These systems are many and varied⁶ but one of them is already implemented to some extent on the reference aircraft: high lift devices blown by propeller slipstream. By blowing the wing with the two 3.93 m propellers, the dynamic pressure over the blown part increases resulting in a lift increment. Of course for a given total thrust, the larger the blown area, the higher the increase in lift coefficient. This technology is fully investigated in the LEAPTech project⁷ in which first results show a maximum lift coefficient in the order of 5.

Neglecting any weight penalty imparted by distributed electric propulsion, the implementation of this technology on the reference aircraft should lead to the improvement of the aerodynamic efficiency in cruise coming from the better positioning of the cruise point along the drag polar but also from the reduction of the wetted area and finally from the increase of the aspect ratio if the wing is resized at iso-span.

However, using multiple propellers along the leading edge in cruise also increases the local Reynolds number on the blown surface which, in turns, increases to some extent the friction drag. Also, the lift distribution over the wing is disturbed by the multiple propeller slipstreams which is to be taken into account during the wing shape optimization. These effects may not fully counterbalance the benefits mentioned previously but are to be considered in the trade study. One alternative solution, also implemented in the SCEPTOR project^{8,9}, consists in folding the small leading edge-mounted propellers not required for cruise propulsion. The split ratio between nacelle-mounted and leading edge-mounted propulsive power can also be optimized (Fig. 9).



Figure 9. SCEPTOR^{8,9}. NASA's Distributed Electric Flight Demonstrator Project.

Also, as the lift gain of a blown wing increases with the thrust, there is no doubt that the blown wing will benefit the take-off field length target. However, concerning approach speed requirement of STOL aircraft (which is the design driver of the wing area of the reference aircraft), approaching the landing field with all propellers at full thrust would require very high and unrealistic angle of attack to keep the approach speed. Still, STOL aircraft fitted with distributed electric propulsion systems such as the one of Fig. 9 can fully benefit from the blown-wing effect in approach and landing by using a particular propeller power management. As suggested in Ref. 10, the power sent to the small leading edge propellers could be that required to ensure the maximum lift coefficient with appropriate stall margin considerations and the two other bigger propellers could be used as needed to keep the -3° approach slope, be it by generating thrust or drag.

In order to assess the effect of a 10% increase in lift capability during approach on the overall energy consumption, the wing area of the aircraft was reduced by 10% at iso-span and the tail surfaces were redesigned at iso-volume coefficients. The drag polar was updated accordingly but neither the characteristic weights nor the

propulsion system were modified. As a result, the block fuel was reduced by 2.5%. Of course, further fuel burn reduction may be achieved with a higher increase in lift capabilities.

Table 12. Summary of “Blown Wing” analysis.

Benefits	▪ -2.5% Block Energy (for only 10% increase in maximum lift coefficient in approach configuration).
Penalties	▪ Additional drag of the folded propellers and their nacelles in cruise.

C. Boundary Layer Ingestion

The theoretical benefit of boundary layer ingestion on propulsive efficiency has been known for several decades and is already implemented in marine propulsion. In the past, various research works have been carried out on the application of the concept to aircraft propulsion and it is now being studied even further as it could be a key concept to make commercial aircraft more energy efficient. There are many different ways of explaining the boundary layer ingestion benefits. The classical explanation is that ingesting a flow with reduced velocity requires less power from the propulsor to create the same amount of thrust. Another view¹¹, is that it reduces the power dissipation in the overall flowfield through the reduction of wasted kinetic energy left by the aircraft by filling the aircraft wake with the propulsor outflow.

A preliminary assessment of boundary layer ingestion for the reference aircraft is presented hereafter. The method used is derived from Ref. 12 and is based on the actuator disk theory. This method may seem simplistic but provides the order of magnitude of potential benefit from a limited number of parameters.

In this study, a propeller is placed behind the fuselage and fully ingests the fuselage wake as in Fig. 7. Let consider that the outlet fuselage control volume is sufficiently far downstream the fuselage for the pressure to be equal to that of the free-stream. Also let assume that iso-momentum mixing occurs within the fuselage wake to deal with a fuselage wake of uniform velocity v_{BL} . Then from momentum considerations, the drag of the fuselage is given by:

$$D_F = \dot{m}_{BL}(v_\infty - v_{BL}) \quad (5)$$

In equation (5), \dot{m}_{BL} is the mass flow rate passing through section CC (Fig. 7) in the boundary layer. The boundary layer thickness as well as the velocity profile along this section have to be known for the calculation of \dot{m}_{BL} . As these data were not directly available, the boundary layer thickness was calculated thanks to the momentum theory within the boundary layer assuming no pressure gradient, which can be formulated as:

$$D_F = \rho 2\tau \int_0^\delta (R_{CC} + r)u(r)(v_\infty - u(r))dr \quad (6)$$

A 1/7 power law velocity profile $u(r)$ for turbulent boundary layer was chosen. Of course the assumption of zero-pressure-gradient boundary layer is not satisfied in reality and pressure distribution should be taken into account in the application of the momentum theory. Also, the 1/7 power law velocity profile assumes that the boundary layer at section CC is fully attached while flow separation probably occurs at the fuselage rear end. However these rough approximations provide a simple way to obtain a first estimation of the boundary layer thickness. Afterward, \dot{m}_{BL} can be calculated by integrating the mass flow rate within the boundary layer at section CC.

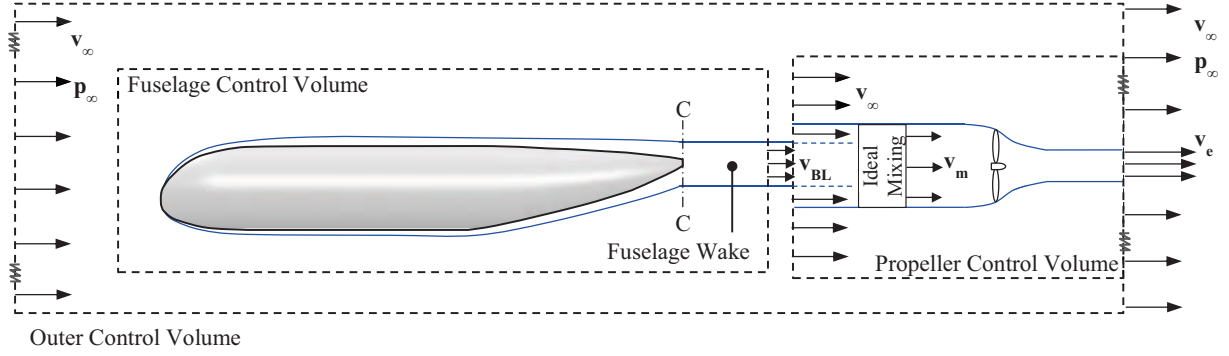


Figure 7. Rear propeller fully ingesting the fuselage wake.

For simplicity the fuselage wake is assumed to mix ideally at the propeller streamtube inlet providing a uniform flow of velocity v_m that is less than the freestream velocity but at least greater than v_{BL} as the propulsor fully ingests the fuselage wake. Applying conservation of momentum in the mixing region yields:

$$\dot{m}_{BL}(v_\infty - v_{BL}) = \dot{m}_p(v_\infty - v_m) = D_F \quad (7)$$

Then, using the actuator disk theory inside the propeller control volume gives the following relations between propeller disk area S_p , propeller thrust T_p and flow properties:

$$T_p = \dot{m}_p(v_e - v_m) \quad (8)$$

$$\dot{m}_p = \rho S_p(v_e + v_m)/2 \quad (9)$$

Finally, the kinetic power imparted to the flow by the propulsor is:

$$P_k = \dot{m}_p(v_e^2 - v_m^2)/2 \quad (10)$$

Therefore, for a given fuselage drag and rear propeller thrust the power provided by the propeller to the flow can be calculated by solving Eqs. (7), (8) and (9). The power defined by Eq. (10) assumes ideal efficiency of the propeller and does not account for friction losses and blade tip losses.

Coming back to the reference aircraft, the potential benefit of boundary layer ingestion was evaluated in cruise. In that phase the fuselage drag represents approximately 16% of the total aircraft drag. In the case when a rear propeller provides 16% of the total thrust, based on the outer control volume of Fig. 7 it can be stated that v_e equals the free stream velocity and the fuselage wake is said fully filled. In order to assess the full benefit of boundary layer ingestion, the thrust sharing between nacelle-mounted propellers and the rear propeller was varied as well as the rear propeller disk loading. The power consumption of the nacelle-mounted propellers was calculated using actuator disk theory with ideal efficiency and their disk loading was kept constant and equal to the reference propeller loading.

The power consumption for the different thrust splits and rear propeller loading were calculated and compared to the power consumption of the non BLI configuration 100/0 (Fig. 11). With the reference disk loading for the rear propeller, all BLI configurations show a benefit of roughly -0.7%. This benefit can be slightly improved by increasing the rear propeller loading for certain thrust combinations only. Analyzing the system of equations solved during this study, it can be seen that for any given rear propeller thrust that is smaller than two times the fuselage drag, the kinetic power provided by the rear propeller decreases as disk loading increases. However, for any given rear propeller thrust that is higher than two times the fuselage drag, the inverse is observed. This explains why it is interesting to reach higher rear propeller disk loading for thrust split configurations 84/16 and 75/25. However, for a given rear propeller thrust, increasing the propeller loading decreases the mass flow rate \dot{m}_p thus approaching the lower bound \dot{m}_{BL} that assures that Eq. (7) is satisfied. This limit was reached with the rear propeller loading increased by 50%. As \dot{m}_{BL} were calculated from rough assumptions, it may be possible to increase the propeller loading even more but the benefit of boundary layer ingestion for these two configurations would probably never

exceed 1%. As the four other thrust split configurations require less power when the rear propeller loading decreases, the disk loading was reduced by 25% versus the reference. If configuration 0/100 shows best propulsive efficiency gain (100% of the thrust is provided by the rear propeller operating in BLI configuration), the associated propeller diameter is 6.5 m. As this propeller diameter raises integration issues, it can be concluded that the benefit of boundary layer ingestion for the reference aircraft would probably never exceed 1% whatever the thrust split ratio. In addition, it can be reminded that the calculation of the power consumption does not account for friction losses, blade tip losses, or unfavorable effect of the distorted propulsor inflow on the propeller performance.

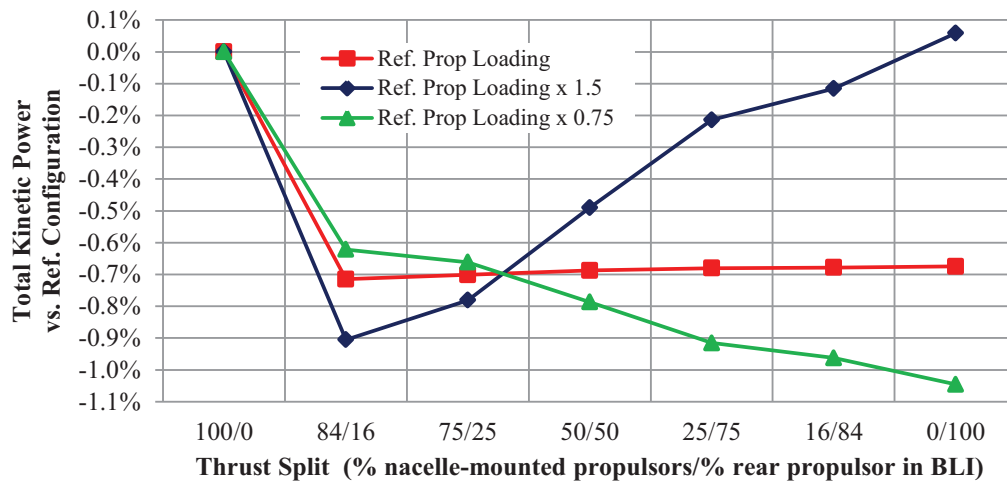


Figure 11. BLI benefits as a function of thrust split ratios.

As propellers already have relatively good propulsive efficiency in freestream, the benefit of boundary layer ingestion is negligible. Fitting the reference aircraft with a rear propeller may provide other benefits such as drag reduction coming from the decrease of nacelle size but also from the reduction of the vertical tail plane as less yaw moment is to be balanced in case of one engine failure. Nevertheless, those benefits are directly related to the propulsion system integration and not to the BLI concept itself.

Table 13. Summary of “Boundary Layer Ingestion” analysis.

Benefits	▪ Less than 1% of propulsive efficiency improvement.
Penalties	▪ Rear propeller integration.

V. Summary and Conclusion

Various technologies enabled by electric power for the purpose of regional aircraft propulsion were analyzed through this article. Table 14 summarizes the benefits at technology level as well as the possible penalties that were pointed out in each study. Also, this table provides an estimation of associated overall energy savings for the 200 nm mission in the most optimistic case, by ignoring any penalty at aircraft level. The calculations are based on the reference aircraft fuel burn (Table 3).

The “Energy Recovering” and “Boundary Layer Ingestion” concepts show negligible benefits on the overall energy consumption that do not justify further investigations on these technologies for our reference aircraft. Even if the “Engine Downsizing” concept shows poorer energy efficiency than the reference aircraft at first sight, the economic aspects have to be considered to come to a conclusion. All other studied technologies show interesting potential energy savings, the implementation cost for some concepts such as “Low Propeller rpm in Taxi” being less than for others such as “Differential Thrust” or “Blown Wing”. Nevertheless, those benefits have to be put in contrast with weight and drag penalties caused by additional electrical components, energy storage devices and possible cooling systems.

The optimization of the hybrid aircraft and the evaluation of its performance require further trade studies that have to be performed with an overall aircraft design loop dedicated to hybrid aircraft. Results of this article can be used as first indicators for selecting the most promising hybrid architecture concepts for a regional aircraft.

Table 14. Results overview.

Technology	Benefits at Technology Level	Max. Block Energy saving (no penalty considered)	Potential Penalties	To be further investigated	Not relevant for our ref. aircraft
Low Propeller rpm in Taxi	<ul style="list-style-type: none"> Propeller efficiency increased by 49%. 	-0.9% BE	<ul style="list-style-type: none"> Non-propulsive systems (including hydraulic power generation) to be rethought. Possible weight penalties imparted by new components (electromechanical actuators, power electronics, etc...). 	X	
Secondary Energy Source for Start and Stop	<ul style="list-style-type: none"> <u>Descent</u>: Energy consumption decreased by 60%. <u>Taxi</u>: Energy consumption decreased by 90%. <i>(Assuming 90% efficiency of the electric system vs. 10% of conventional gas turbine in ground idle.)</i> 	<u>Descent</u> : -4.3% BE <u>Taxi</u> : -2.4% BE	<ul style="list-style-type: none"> Non-propulsive systems to be redesigned (Environmental Control System, Anti-icing, etc...). Additional weight of secondary energy source. 	X	
Single Engine Aircraft	<ul style="list-style-type: none"> Prime mover efficiency increased by 10.5%. 	-7.8% BE (only climb and cruise considered)	<ul style="list-style-type: none"> Additional weight of back-up system. 	X	
Engine Downsizing	<ul style="list-style-type: none"> Lower maintenance costs. Easier engine integration. 	n/a	<ul style="list-style-type: none"> Prime mover efficiency reduced by 0.5%. Additional weight of secondary power generation system. 	X	
Energy Recovering	<ul style="list-style-type: none"> Energy recoverable at landing=0.2% BE. 	-0.2% BE	<ul style="list-style-type: none"> Increased Block Energy for energy recovering in descent. System complexity for kinetic energy recovering at landing. Additional weight of energy recovering systems. 		X
Differential Thrust	<ul style="list-style-type: none"> Reduced skin friction drag. 	-6% BE (fin fully removed)	<ul style="list-style-type: none"> Reduced aircraft natural stability. 	X	
Blown Wing	<ul style="list-style-type: none"> Increased lift-to-drag ratio in cruise. 	-2.5% BE (for only 10% increase of max. lift coefficient)	<ul style="list-style-type: none"> Additional drag of the folded propellers and their nacelles in cruise. Weight of the powered high-lift system. 	X	
Boundary Layer Ingestion	<ul style="list-style-type: none"> Increased propulsive efficiency (less than 1%). 	-0.8% BE (only climb and cruise considered)	<ul style="list-style-type: none"> Rear propeller integration. 		X

References

- ¹Hamilton Standard, "Generalized Method of Propeller Performance Estimation," Hamilton Standard PDB6101, 1963.
- ²Marconi, P., Serghine, C., "Alternative Method for Re-starting a Helicopter Turboshaft Engine on Standby, and Multi-engine Helicopter Propulsion System Allowing such a Method to be Performed," TURBOMECA Patent WO/2015/145036, 2015.
- ³Roth, B., Giffin, R., "Fuel Cell Hybrid Propulsion Challenges and Opportunities for Commercial Aviation," *46th AIAA/ASME/SAE/ASEE Joint Propulsion Conference & Exhibit*, AIAA, Nashville, TN, July 2010.
- ⁴Thauvin, J., Barraud, G., Roboam, X., Sareni B., Budinger, M., Leray, D., "Hybrid Propulsion for Regional Aircraft: a Comparative Analysis based on Energy Efficiency," *International Conference on Electrical Systems for Aircraft, Railway, Ship Propulsion and Road Vehicles (ESARS)*, IEEE, Toulouse, 2016. Submitted for publication.
- ⁵Armstrong, M., Ross, C., Phillips, D., Blackwelder, M., "Stability, Transient Response, Control, and Safety of a High-Power Electric Grid for Turboelectric Propulsion of Aircraft," NASA/CR-2013-217865, 2013.
- ⁶Petrov, A. V., "Aerodynamics of STOL Airplanes with Powered High-Lift Systems," *28th International Congress of the Aeronautical Science*, ICAS, 2012.
- ⁷Stoll, A. M., "Comparison of CFD and Experimental Results of the LEAPTech Distributed Electric Propulsion Blown Wing," *15th AIAA Aviation Technology, Integration, and Operations Conference*, AIAA, Dallas, TX, June 2015.
- ⁸Patterson, M. D., Derlaga, J. M., Borer, N. K., "High-Lift Propeller System Configuration Selection for NASA's SCEPTOR Distributed Electric Propulsion Flight Demonstrator," *16th AIAA Aviation Technology, Integration, and Operations Conference*, AIAA, Washington, D.C., June 2016.
- ⁹Dubois, A., Geest, M., Bevirt, J., Clarke, S., Christie, R. J., Borer, N. K., "Design of an Electric Propulsion System for SCEPTOR," *16th AIAA Aviation Technology, Integration, and Operations Conference*, AIAA, Washington, D.C., June 2016.
- ¹⁰Stoll, A. M., Mikic, G. V., "Design Studies of Thin-Haul Commuter Aircraft with Distributed Electric Propulsion," *16th AIAA Aviation Technology, Integration, and Operations Conference*, AIAA, Washington, D.C., June 2016.
- ¹¹Uranga, A., Drela, M., Greitzer, E. M., Titchener, N. A., Lieu, M. K., Siu, N. M., Huang, A. C., "Preliminary Experimental Assessment of the Boundary Layer Ingestion Benefit for the D8 Aircraft," *52nd Aerospace Sciences Meeting*, AIAA, National Harbor, MD, January 2014.
- ¹²Rodriguez, D. L., "A Multidisciplinary Optimization Method for Designing Boundary Layer Ingesting Inlets," Ph.D. Dissertation, Aeronautics and Astronautics Dept., Stanford Univ., January 2001.